The impact of urban vegetation morphology on urban building energy consumption during summer and winter seasons in Nanjing, China

Sijie ZHU[a], Yanxia LI[a], Shen WEI[b], Chao WANG[a], Xinkai ZHANG[c,d], Xing JIN[a], Xin ZHOU[a], Xing SHI[*c,d]

[a] School of Architecture, Southeast University, Nanjing, China; zhusijie@seu.edu.cn (Z. S.); liyanxia@seu.edu.cn (L. Y.); 230189011@seu.edu.cn (W. C.); x.jin@seu.edu.cn (J. X.); 101012014@seu.edu.cn (Z. X.)

[b] The Bartlett School of Sustainable Construction, University College London, London, WC1E7HB, UK; shen.wei@ucl.ac.uk

[c] College of Architecture and Urban Planning, Tongji University, Shanghai, China; zhangxinkai@tongji.edu.cn (Z. X.);

[d] Key Laboratory of Ecology and Energy-saving Study of Dense Habitat (Tongji University), Ministry of Education, China

*Correspondence: 20101@tongji.edu.cn; Tel.: +86 15905191490

Abstract:

Studies have shown that urban vegetation can be an effective strategy for reducing energy consumption in urban buildings by regulating the microclimate and shading solar radiation on building surfaces. However, an understanding of the potential energy savings of vegetation morphological planning at the urban scale is still lacking, particularly regarding the quantitative correlation between urban vegetation morphology and its impact on urban building energy use. The morphology of the metropolitan area in Nanjing, a typical hot summer/cold winter city in eastern China, was statistically analyzed, and 40 urban building-vegetation morphological prototypes were extracted. Using the proposed co-simulation technique for urban microclimate and urban building energy, the summer and winter building energy consumption of the prototypes were simulated. A quantitative analysis was conducted on the relationship between urban vegetation morphology indexes and building energy consumption. The results indicate that strategically planned urban vegetation morphology can significantly reduce urban building energy consumption. In the summer, vegetation close to the geometric center of the site, uniformly distributed and highly mixed with buildings, can significantly reduce the building energy consumption; in the winter, the opposite is true. The presented findings provide designers and planners with strategies for incorporating urban vegetation morphology design into the construction of energy-efficient cities.

1 Introduction

Urban areas are associated with more than 67% of energy consumption and 71% of associated greenhouse gas emissions (Seto et al., 2014). Space conditioning and lighting for urban buildings account for over 40% of the total energy use in the US (US Department of Energy, 2015). Lighting, space cooling and appliances account for 30%, and space heating accounts for 32% of China's buildings sector final energy consumption (excluding biofuels) (IEA, 2015). Therefore, for sustainable development, efforts need to be made to improve the energy performance of buildings, and measures from urban planning and management to improve the efficiency of building energy use are one focus of current research (Natanian & Auer, 2020; Shi et al., 2017; Tian et al., 2018).

Among the many parameters influencing building energy, vegetation morphology is critical (Ko, 2018). Numerous studies have confirmed that strategic planning of vegetation morphology can shade the solar radiation absorbed by walls in summer and block the infiltration of cold wind as windbreaks in winter, thus saving the cooling and heating energy to a great extent (Heisler, 1986; Meier, 1990; Pan et al., 2018; Simpson, 1998). Since the cooling intensity of vegetation is affected by its size, spatial pattern and canopy type, its energy-saving efficiency is affected by these characteristics (Balogun et al., 2014; Du et al., 2017; Hwang et al., 2016). The relative location of shade vegetation to the building is another factor affecting buildings' energy consumption. In most cases, the shade vegetation on the west and south sides of the building helps to keep buildings cool and shows energy efficiency in summer, while the vegetation on the north side increases the energy use (Donovan & Butry, 2009; Hildebrandt & Sarkovich, 1998; Ko & Radke, 2014; Pandit & Laband, 2010). In colder cities requiring more heating, vegetation in the south of the building even significantly increases the annual energy consumption because the tree shade blocks passive solar heating (Thayer et al., 1983). In cold and windy weather, urban vegetation in upwind areas forms windbreaks to slow winter monsoons and consequently reduce infiltration for less heat loss from buildings (DeWalle & Heisler, 1983). Additionally, the canopy size, shape, distribution density, and distance from the building affect building energy consumption (Hildebrandt & Sarkovich, 1998; Simpson, 2002). The effect of vegetation on building energy also depends on tree species. Compared with deciduous trees, conifers block passive solar heating and cause a more significant winter energy loss (Ko, 2018). Table 1 shows several vegetation morphological features affecting building energy confirmed in the existing literature.

Table 1

Several vegetation morphological features affecting building energy, as shown in the literature.

Reference	Location	Climate	Season	Vegetation feature	Impact on building energy
(Pandit & Laband, 2010)	Auburn, Alabama	Humid Subtropical Climate	Summer	Tree shade density	Dense shading significantly provides more cooling. In a "typical" house with a moderate shadow coverage of 19.3%, dense shadows reduce daily electricity consumption by an estimated 9.3%.
(Donovan & Butry, 2009)	Sacramento, California	Hot-summer Mediterranean climate	Summer	Relative position to building	In the eastern quadrant of the building, the positive and negative effects of trees on energy offset each other, while in the southern and western quadrants, the energy-saving effect of trees is dominant.
(Hwang et al., 2016)	Four US Cities: Minneapolis, Indianapolis, Charlotte, and Orlando	Hot-summer humid continental climate and humid subtropical climate	Summer and winter	Size and relative position to building	The best performing scenes are medium and large trees on the west side, followed by the east and south sides. Trees on the north side have a limited impact on annual energy. Compared with deciduous trees, conifers cause heating losses in winter.
(Ko & Radke, 2014)	Sacramento, California	Hot-summer Mediterranean climate	Summer	Density, height, and relative position to the building	The higher vegetation density within a certain distance and the sum of the tree heights on the east, south, and especially on the west side of the house have a statistically significant impact on building energy and help to reduce the use of cooling energy.
(Simpson & McPherson, 1996)	California	Representative cooling dominated climates in the US, except for the hot/humid southeast.	Summer and winter	Size, relative direction to the building and the distance from the building	The trees on the west side provide the best energy-saving benefits, followed by the southwest and east. As the distance from the building to the tree increases, the shading effect decreases. Tall trees near the south wall increase energy consumption in winter.

Urban vegetation directly or indirectly affects urban building energy flow factors, including heat conduction of building envelope, air exchange and heat increment caused by solar radiation. Figure 1 illustrates the main influence paths of vegetation on building energy flow. The shading effect of vegetation directly reduces the solar heat increment absorbed by windows, walls and roofs (Donovan & Butry, 2009; Hwang et al., 2016; Pan et al., 2020; Pandit & Laband, 2010). Another way in which vegetation affects energy in urban buildings is by influencing the microclimate between the building surface and the adjacent vegetation (Du et al., 2022; Meier, 1990; Zhu et al., 2022). Specifically, urban vegetation affects building energy through the following microclimate processes: a) cooling the external air temperature of buildings through the incident solar radiation response and latent heat loss caused by transpiration and canopy interception and thus reduces the envelope heat gain transferred by convection; b) reducing the solar radiation gain of man-made surface features of the region thereby reducing the longwave radiation received by the building envelope and the air temperature increases from convective heat transfer; c) increasing the air humidity around the building, and this may cause a moderate reduction in thermal comfort, thus increasing cooling or heating energy demand (Scott et al., 1994) ; d) decreasing the local wind speed by increasing the length of urban surface roughness, resulting in a reduction in the convection coefficient on the wall surface and air infiltration (Heisler, 1990; McPherson & Rowntree, 2016; Meier, 1990). In addition, vegetation may affect energy-related occupant behavior, such as time spent outdoors (Schipperijn et al., 2013), thermal comfort perception (Mangone et al., 2014) and window operating behavior (Liu et al., 2022), and thus affect the building's energy consumption (Hong et al., 2016; Zhou et al., 2018; Zhou et al., 2021).

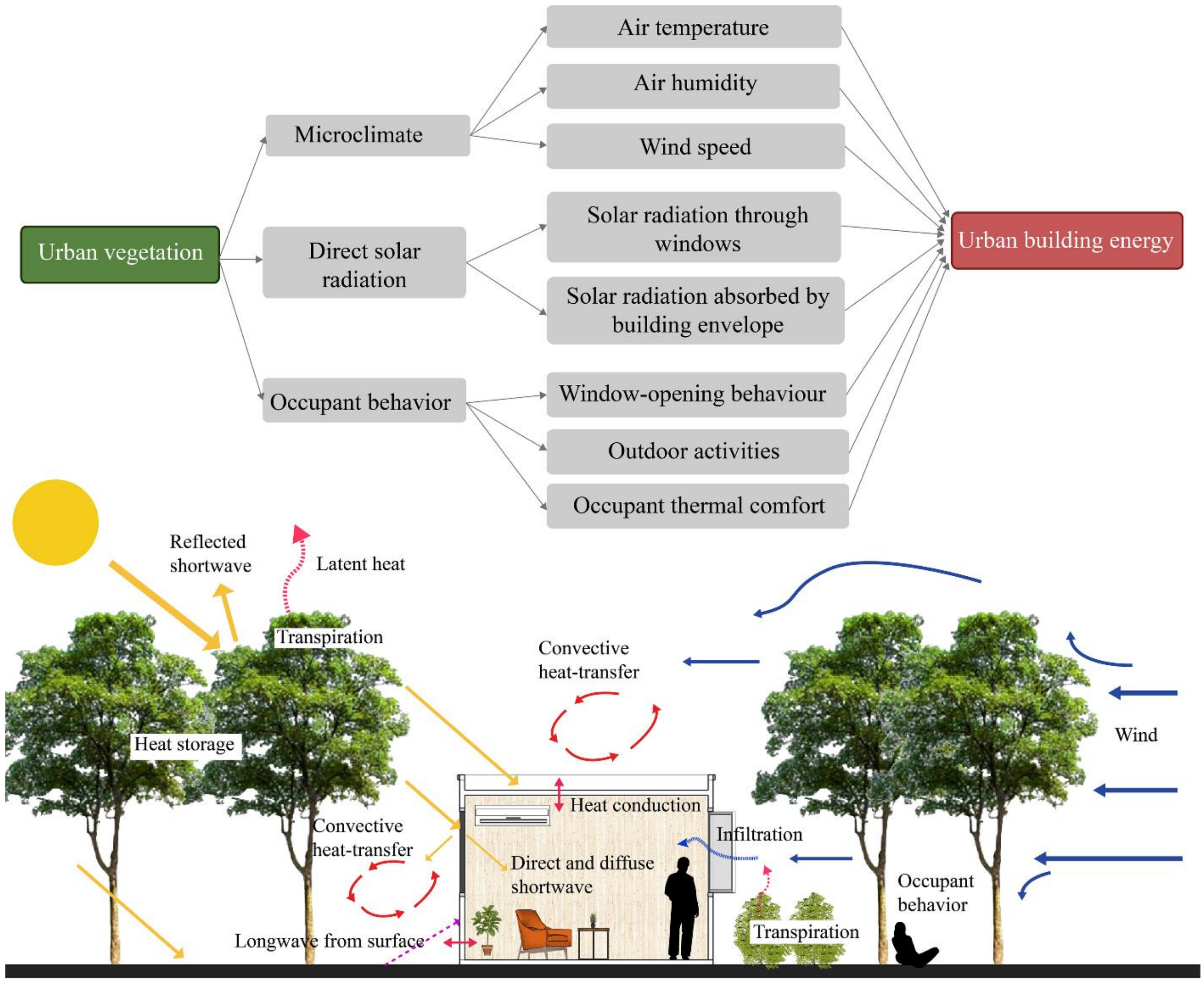

Fig. 1. The influential mechanism of urban vegetation on building energy flow.

The influence of urban vegetation on building energy at the individual building level has been proven in numerous existing studies, and its mechanism has been well understood. However, there is a lack of understanding of the relevance between urban vegetation morphology and urban building energy on an urban scale, especially the quantitative correlation. The research at the individual building level cannot reflect how the widely existing public greenspace form and the spatial structure of urban vegetation affect the energy usage of urban buildings and its affecting magnitude. Urban vegetation morphology, as an important tool for urban planning and management, reflects the physical geometry, internal composition and spatial structure of the vegetation widely distributed in urban public spaces. The application of a regular understanding of the relationship between urban vegetation morphology and urban building energy to urban design and management is conducive to the energy conservation of the vast quantities of buildings in cities, resulting in a significant energy benefit.

This paper presents a quantitative analysis of the correlation between urban building energy and urban vegetation morphology. A co-simulation technique for urban microclimate and urban building energy has been developed. Based on the statistical analysis of the building and vegetation morphology in the metropolitan area in Nanjing, China, the urban building-vegetation morphological prototypes were summarized and refined. Applying the prototypes and co-simulation technique, the influence of various morphological parameters of vegetation on urban building energy was statistically analyzed. Based on summarized findings, a general low-energy-oriented vegetation morphological strategy was proposed.

2 Methodology

2.1 Case study area and meteorological data

Nanjing is one of the central cities in China's Yangtze River Delta Region. It is in the subtropical monsoon humid climate zone, with four distinct seasons, abundant rainfall and sufficient sunlight. Nanjing has a typical hot summer and cold winter climate. The heating season is roughly as long as the cooling season. The vegetation of Nanjing is mixed deciduous and broad-leaved evergreen, dominated by deciduous tree species (Jim & Chen, 2003). The metropolitan area of Nanjing, 108.97 km^2, was selected for urban morphology analysis. The area encompasses 952 urban blocks, excluding those without buildings (undeveloped areas or parks). Eighty-six blocks were used to investigate the volume of vegetation canopy. Figure 2(a) illustrates the location of Nanjing and the metropolitan area selected for the study.

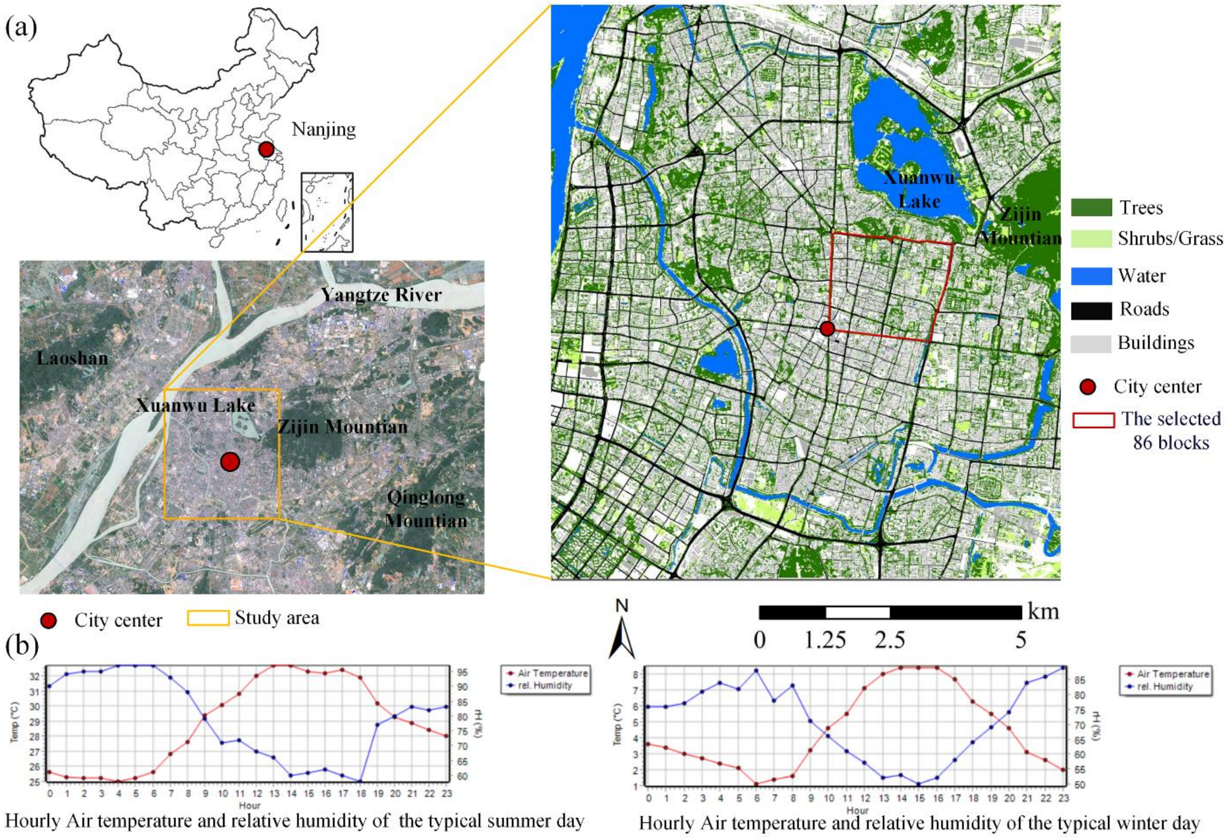

Fig. 2. (a) The location of Nanjing and the selected metropolitan area for the study; (b) the meteorological data of the typical summer and winter days.

The meteorological data in a typical meteorological year (TMY) in Nanjing were analyzed to select typical weather days. Two selection rules were followed: (a) the daily temperature, humidity, wind speed, and direction are close to the mean values of the season; (b) the diurnal variation of air temperature and humidity is close to that of the season. According to these rules, July 27 was selected as the typical summer day, and February 17 the typical winter day (Figure 2(b)). The hourly weather data of the typical summer and winter days were used to simulate the urban microclimate and building energy consumption.

2.2 Prototypes of urban vegetation morphology

The morphology of the urban blocks in the study area was statistically analyzed to develop the building-vegetation morphological prototypes. These prototypes were then simulated to evaluate the urban building energy use.

2.2.1 The scale of the prototypes

In urban spaces, the air needs a certain distance to gradually adapt to new boundary conditions when flowing between adjacent areas. Under the underlying urban surface and atmospheric conditions, the adjustment distance of the air at the height of the louver is no less than 200 m (Oke, 2002; Stewart & Oke, 2012). In addition, the average block size is 93698 m^2 in the study area. Taking into account the adjustment distance of the air and the block scale, the size of the prototype was set to be 600 × 600 m, equal to the size of four blocks.

2.2.2 Classification of basic types

The building height, building density and greening ratio were statistically analyzed to summarize the basic types of urban morphology. The data, including the building plane profile and height, was from the Baidu map obtained using crawler technology. The data format was ShapeFile for spatial statistics in GIS (Geographic Information System). High-rise blocks were defined as those with an average building height of more than 24 m; low-rise blocks less than 24 m. The median building densities of high-rise blocks and low-rise blocks were calculated to be the thresholds for high-density and low-density blocks. Using the remote sensing data of the GF-2 satellite(Chen et al., 2022), the vegetation in the study area and its coverage ratio in each urban block were classified and statistically analyzed. Figure 3 shows the building density and greening ratio statistics of the study blocks. A block with a greening ratio higher than the median value was defined as a high greening ratio block and vice versa. Table 2 shows the eight basic urban morphological types and their proportions.

Table 2

The classification of eight basic urban morphological types and the proportion of blocks in the study area.

Height type	Height	Density type	Density	Green coverage type	Greening ratio	Block number	Percentage
Low-rise	< 24 m	Low	< 0.28	High	> 0.23	246	25.84%
				Low	< 0.23	92	9.66%
		High	> 0.28	High	> 0.23	107	11.24%
				Low	< 0.23	231	24.26%
High-rise	> 24 m	Low	< 0.27	High	> 0.23	99	10.40%
				Low	< 0.23	39	4.10%
		High	> 0.27	High	> 0.23	24	2.52%
				Low	< 0.23	114	11.97%

Three-dimensional vegetation morphology plays a vital role in urban environmental regulation (Zhu et al., 2020). Therefore, the crown size of vegetation in 86 blocks (shown in Figure 2(a)) was statistically analyzed. The selected area is located between the city center and two important natural ecosystems in Nanjing, namely the Zijin Mountain and the Xuanwu Lake, reflecting a transition from the high-density and low-greening coverage morphology to the low-density and high-greening coverage morphology. Since this transition is quite common in Nanjing, it is of representative significance to the urban morphology of the city. The CVI (Crown Volume Index) data acquisition method is included in the Supplementary Information. The CVI is defined as the canopy volume per unit area of the crown projection, with a median value of 8.59 m^3/m^2 in the investigated blocks (Figure 3).

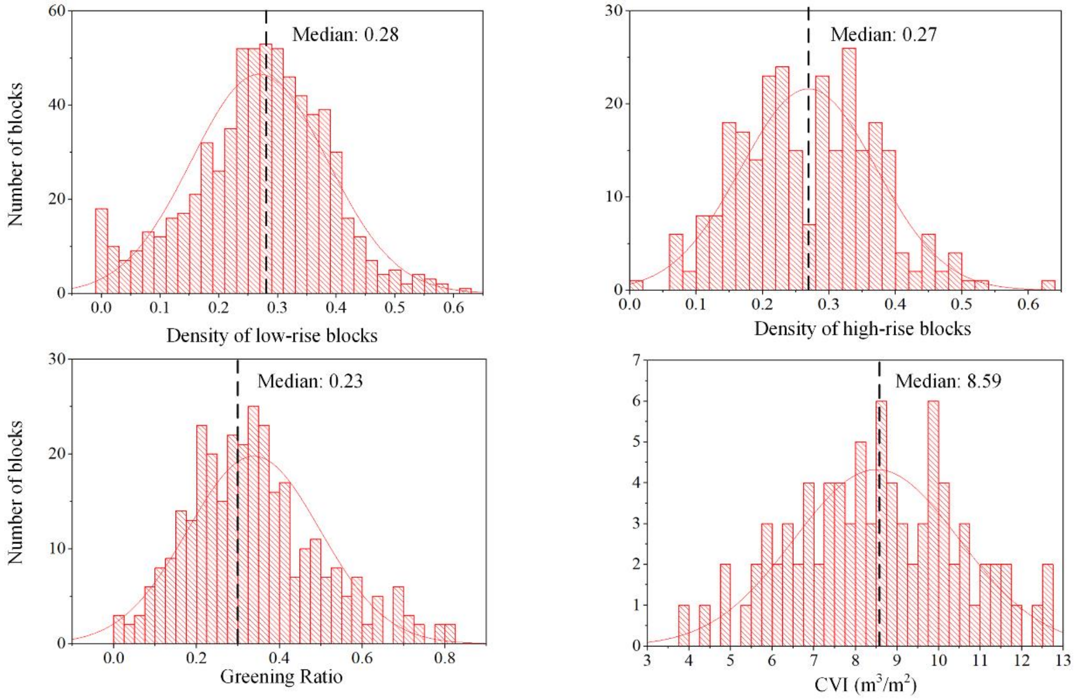

Fig. 3. The statistical results of building height, density, greening ratio and CVI in blocks of the study area.

The median value of the height and density types were adopted as the parameters-settings of the prototypes. Table 3 shows the morphological parameters of the eight basic types: LLL (low-rise, low-density, and low-greening ratio), LLH (low-rise, low-density, and high-greening ratio), LHL (low-rise, high-density, and low-greening ratio), LHH (low-rise, high-density, and high-greening ratio), , HLL (high-rise, low-density, and low-greening ratio), HLH (high-rise, low-density, and high-greening ratio), HHL (high-rise, high-density, and low-greening ratio) and HHH (high-rise, high-density, and high-greening ratio). Since three basic types, namely LLL, HLL and HHH, are proportionally low, each accounting for less than 10% of all blocks, they were not included in the prototypes. The other five basic types, accounting for 83.7% of all blocks, were determined to be the prototypes for simulation (Figure 4).

Table 3

Morphological parameters of the 8 basic types.

Basic type	Building height (m)	Building density	Crown volume (m^3)
LLL	16	0.18	313295
LLH	16	0.18	778016
LHL	16	0.36	313295
LHH	16	0.36	778016
HLL	35	0.18	313295
HLH	35	0.18	778016
HHL	35	0.35	313295
HHH	35	0.35	778016

Deciduous trees dominate the study area, accounting for nearly 84% of all vegetation. Conifers are nonexistent in most blocks and therefore not considered. *Cinnamomum camphora* is the most representative evergreen species, accounting for 56% of the crown volume of evergreen trees. *Platanus acerifolia* is the dominant deciduous species, accounting for 84% of the deciduous crown volume. The average sizes of the two representative tree species were extracted and integrated into the five prototypes (Table 4).

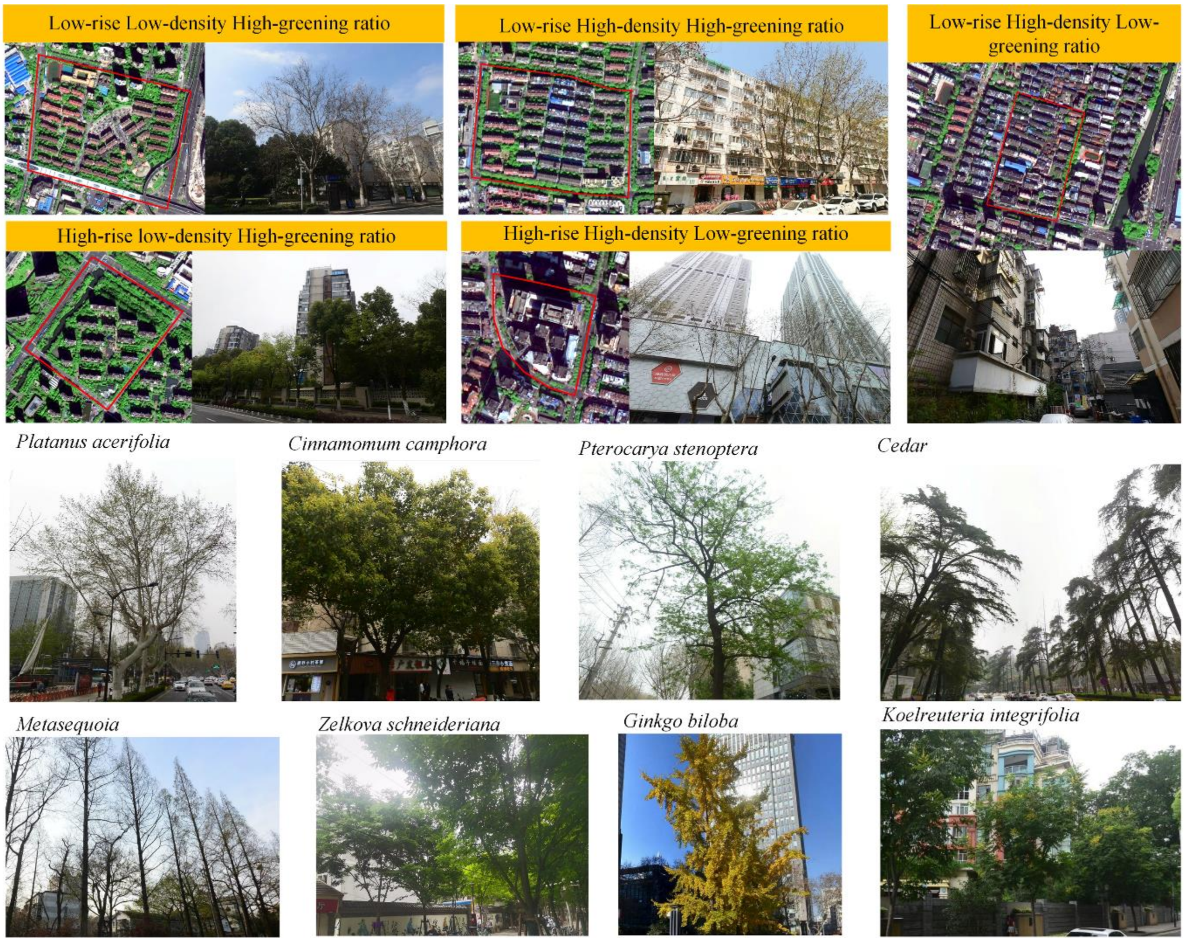

Fig. 4. Typical blocks of five selected basic types and representative tree species in the study area.

Table 4

The statistical average sizes and grid sizes of representative tree species in the study area.

Category	Representative specie		Crown width (m)	Crown height (m)	Height to the crown base (m)
Deciduous	Platanus acerifolia	Statistical size	17.78	18.81	8.17
		Grid size	16	16	8
Nondeciduous	Cinnamomum camphora	Statistical size	8.50	9.12	4.28
		Grid size	8	8	4.8

The values include the statistical size and grid size, where grid size is the value used in the ENVI-met model. The tree crowns were simplified and modeled as cubes.

2.2.3 Classification of spatial types

As shown in Figure 5, the spatial distribution of vegetation in a basic type has 8 variations. By combining 5 block prototypes with 8 vegetation spatial distributions, 40 building-vegetation morphological prototypes were obtained. They were later simulated to study the correlation between urban building energy and morphology.

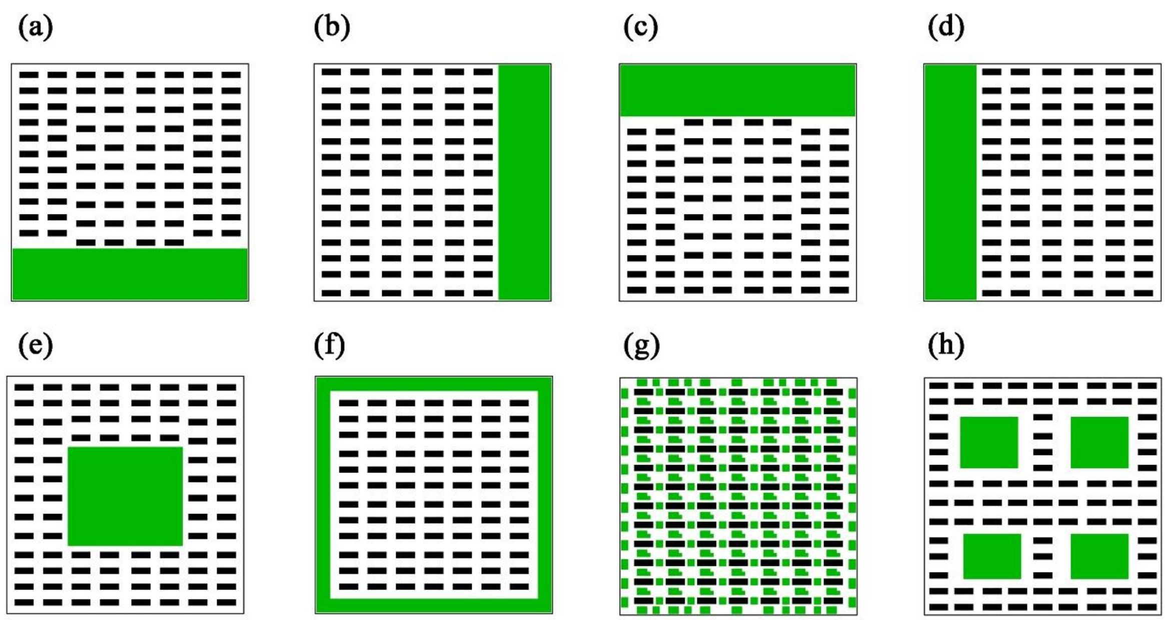

Fig. 5. Eight vegetation spatial distribution in the LLH type including (a) south-concentrated, (b) east-concentrated, (c) north-concentrated, (d) west-concentrated, (e) middle-concentrated, (f) surrounding, (g) uniform and (h) grouping.

2.3 Co-simulation technique combining vegetation, microclimate and urban building energy

2.3.1 Simulation tools of microclimate and building energy

ENVI-met 4.4.5 was used in the microclimate simulation. ENVI-met is a numerical simulation model for urban microclimate. Based on the hydromechanics and thermodynamic equations, the model simulates the "surface-vegetation-atmosphere" interaction with a spatial resolution of 0.5-10 meters (Bruse, 2004; Bruse & Fleer, 1998). A unique feature of ENVI-met is detailed vegetation modeling, which takes into account the interaction between vegetation and atmosphere, including transpiration, evaporation and sensible heat flux. In addition, the simulation considers water and heat exchange inside the soil, including plant water uptake. ENVI-met is widely used to predict the effect of urban vegetation on microclimate and validated by previous studies (Liu et al., 2021; Shinzato et al., 2019; Simon et al., 2018). Table 5 shows the initialization parameter of the outdoor micro-climate model based on the TMY data for both seasons in this study.

Table 5

Simulation parameter settings in ENVI-met.

	Simulation parameters	**Settings**	**Simulation parameters**	**Settings**
	Location	Nanjing, China	Meteorological mode	Simple Forcing
	Simulation start time	00:00	Simulation end time	24:00
	Model area (m)	632× 632 × 72	Spatial resolution (m)	8.00 × 8.00 ×6.00
	Model rotation (°)	0.00 – North	Nested grids (m)	40
Summer	Simulation day	27.07.2022	Wind direction (0 = North)	83.21 (hourly average value)
	Wind speed at 10m above the ground (m / s)	1.96 (hourly average value)	Air temperature (°C)	25.00-32.70
	Relative humidity (%)	58.00-97.00		
Winter	Simulation day	17.02.2022	Wind direction (0 = North)	123.50 (hourly average value)
	Wind speed at 10m above the ground (m / s)	2.63 (hourly average value)	Air temperature (°C)	1.10-8.40
	Relative humidity (%)	50.00-89.00		

EnergyPlus developed by the U.S. Department of energy is widely used in the field of building energy simulation (Fumo et al., 2010; Zhu et al., 2013). By inputting the site weather data, building physical features and related equipment parameters, EnergyPlus simulates the cooling and heating load of buildings through a heat balance model. The heat balance model considers the combined effect of radiation on the building surface and convection (Crawley et al., 2001). EnergyPlus was proved to be more accurate than other commercial energy modeling programs in simulating the building heat load of various buildings (Zhu et al., 2013). EnergyPlus 9.0.1 was used in the building energy simulation. The specific parameter values used in the simulation are shown in Table 6. Residential and office building prototypes were simulated and analyzed separately. The energy consumption on weekdays and weekends was simulated for residential buildings. The weighted average of the building energy consumption on weekdays and weekends was used for the analysis.

Table 6

Simulation parameter settings in EnergyPlus.

Building Type	Glazing Ratio				Lighting Load (w/m^2)	Equipment Load (w/m^2)	Occupant Density (people/m^2)	Infiltration (m^3/s·m^2)	Ventilation (m^3/s·m^2)	Temperature Control Points
	East	South	West	North						
Residential Building	0.17	0.22	0.07	0.19	7	4.30	0.050	0.00025	/	26℃ (Cooling) / 20℃ (Heating)
Office Building	0.17	0.30	0.07	0.25	10	7.64	0.325	0.00021	0.0002	

2.3.2 Co-simulation of urban microclimate and urban building energy.

Previous studies implemented the integration of ENVI-met and EnergyPlus at the individual building level (Morakinyo et al., 2016; Yang et al., 2012). However, due to the complexity of data format conversion among platforms, there is still a lack of workflows for urban-scale simulation.

The modeling, simulation, and interaction processes of ENVI-met and EnergyPlus were integrated into the Rhino and Grasshopper platforms to realize the co-simulation of urban microclimate and energy (Figure 6). The geometric data for urban buildings and vegetation are read from the Shapefiles in GIS. The workflow includes the model and parameter importing module, the microclimate simulation module, the meteorological file conversion module, and the energy simulation module. The model and parameter importing module reads geometric and nongeometric inputs and implements transformations among modules. The microclimate simulation module reads models of buildings and vegetation to simulate the urban microclimate. The meteorological file conversion module analyzes the average microclimates around each building from the ENVI-met output and converts them into EPW files corresponding to each building using an EnergyPlus weather data files (EPWs) generator. The energy simulation module reads the EPW file of each building to simulate the urban building energy in EnergyPlus. The environmental models of surrounding buildings and vegetation are read to simulate radiation transfer to building surfaces. The buildings and vegetation within 100 meters of the building are automatically selected as context before the energy simulation of each building to improve the efficiency of the simulation of solar radiation shading. The simulation results of each building are returned to GIS and connected with the building models for further spatial analysis and visualization.

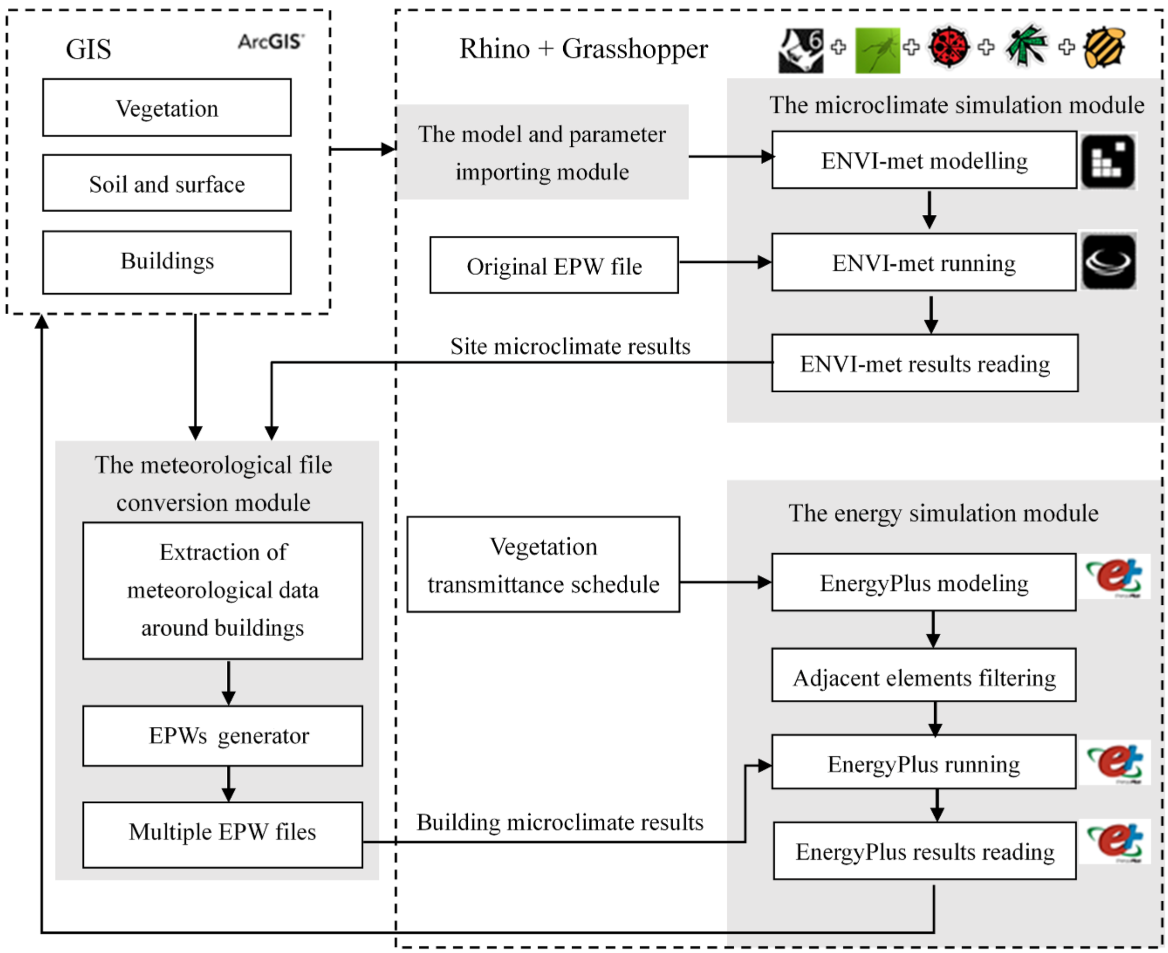

Fig. 6. The co-simulation workflow of urban microclimate and urban building energy.

Weather data in EnergyPlus is input as the standard EPW format. The default EPW data include the hourly air temperature, humidity, wind speed, and solar radiation for a typical meteorological year measured from local weather stations. However, the impact of urban form, including UGI, on microclimate cannot be reflected by the standard EPW (Morakinyo et al., 2017). This study, therefore, replaces the corresponding values in the EPW for each building with the air temperature, relative humidity, and wind speed derived from the ENVI-met simulation results. According to the EnergyPlus input reference (U.S. Department of Energy, 2021), air temperature and humidity in the EPW are measured at a height of approximately 1.5 m above the ground, while wind speed is measured at a height of 10 m above the ground. The microclimate data extracted from ENVI-met simulation results include the average air temperature (1.5m height), average air humidity (1.5m height), and average wind speed (10m height) of adjacent grids of each building. The

EPWs generator converts the meteorological data around buildings into multiple EPW files (Figure 7(a)). By replacing the EPW for each building, it is possible to observe the effect of UGI-induced microclimate changes on the energy consumption of each building in the output of EnergyPlus (Figure 7(b)).

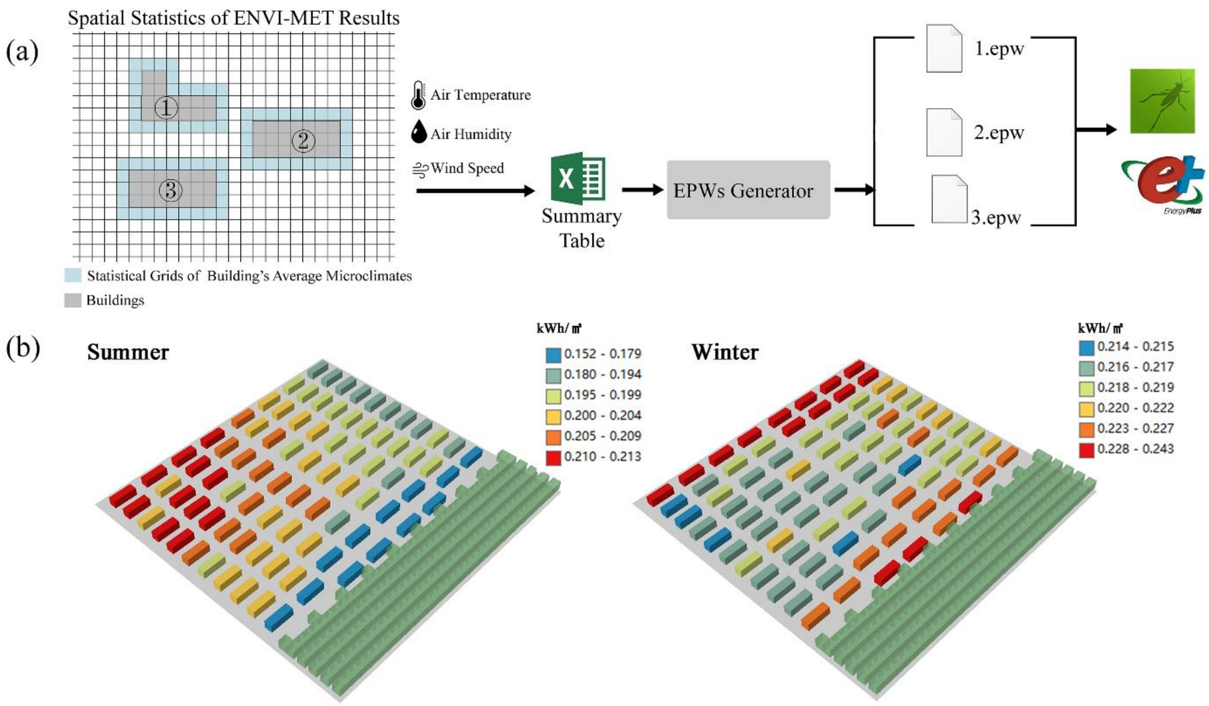

Fig. 7. (a) The method of coupling ENVI-met results into EnergyPlus; (b) simulation results of spatially distributed daily building energy consumption.

2.3.3 Time-dependent vegetation model in urban building energy simulation

An important step in calculating the influence of urban vegetation on the solar radiation shielding of building surfaces is to obtain the transmittance of vegetation. In the geometric modeling of EnergyPlus, the context vegetation was set as surfaces with transmittance. The canopy transmittance of representative tree species in Nanjing on the typical weather days was obtained through the FLiESvox model. FLiESvox is a radiative transfer model for vegetation used to simulate the absorbed PAR (photosynthetically active radiation) (Kobayashi, 2012; Kobayashi & Iwabuchi, 2008). The FliesVox model converts tree crowns into multiple voxels. Each voxel's absorbance to solar radiation is determined by its leaf area density. The approximate transmittance of the tree crown was calculated from the photosynthetically active radiation (PAR) absorbed by each voxel and transferred to the ground. The canopy transmittance on February 17 for average size Platanus acerifolia and Cinnamomum camphora in the study area was 0.83 and 0.64, and that on July 27 was 0.39 and 0.58.

2.3.4 Numerical model validation

The accuracy of outdoor (ENVI-met model) and indoor (EnergyPlus model) simulation was validated by comparing the simulation and measurement in the Sipailou Campus of Southeast University. The Campus is one of the selected eighty-six blocks. The field survey was conducted on February 19, 2022, in a classroom on the first floor of a campus building. The classroom and its adjacent classrooms were kept vacant in the measurement to eliminate the influence of occupant and equipment factors on the indoor temperature. Sensors for temperature, humidity, and wind speed were set at a height of 1.5m near the outer wall of the monitored room. Another temperature sensor was set inside the monitored room. The simulation and measurement of hourly indoor and outdoor temperatures were compared.

The meteorological parameters of microclimate simulation were input from the data of the local meteorological stations. The modeling in ENVI-met and EnergyPlus is shown in Figure 8(a) and Figure 8(c). The monitored room includes an exterior wall with two windows. Figure 8(b) shows the five trees and a lawn adjacent to the exterior wall, including three camphor trees, one palm and one cedar. The main input parameters of ENVI-met are summarized in Table 7. In EnergyPlus, the input meteorological parameters were the measured air temperature, relative humidity, and wind speed of the outdoor monitoring point. The occupant density, equipment, and lighting load were set to zero. Infiltration was set to 0.00021 ($m^3/s\cdot m^2$). The main material of the exterior wall is brick masonry with thermal conductivity of 0.38 w/(m·K).

Table 7

Simulation parameter settings in ENVI-met.

Simulation parameters	**Settings**	**Simulation parameters**	**Settings**
Simulation day	19.02.2022	Simulation start time	00:00
Simulation end time	24:00	Meteorological mode	Simple Forcing
Wind speed at 10m above the ground (m / s)	3.44 (hourly average wind speed from the meteorological station)	Air temperature and relative humidity	hourly average values from the meteorological station
Location	Nanjing, China	Wind direction (0 = North)	1.55 (hourly average wind direction from the meteorological station)
Model area (m)	320 × 320 × 212	Spatial resolution (m)	4.00 × 4.00 ×4.00
Model rotation (°)	0.00 – North	Nested grids (m)	40

Figure 8(d) compares the measured and simulated air temperatures at outdoor and indoor monitoring points for 14 hours from 6:00 (before sunrise) to 19:00 (after sunset) on February 19. For the outdoor temperature, the absolute errors between the measured and the simulated air temperature range from 0.14 ° C to 0.76 ℃, and the root mean squared error (RMSE) is 0.49 ℃. The hourly average temperature of the ground meteorological station is 0.88 ℃ lower than the measured value. Compared with the data from the meteorological station, the simulation results reflect the impact of buildings and vegetation surrounding the building. For the indoor temperature, the absolute error between the measured and the simulated air temperature is 0.01 ° C to 0.21 ℃, and the RMSE is 0.12 ℃. The comparison results validate that the numerical method of microclimate and building energy consumption simulation is reasonable and feasible.

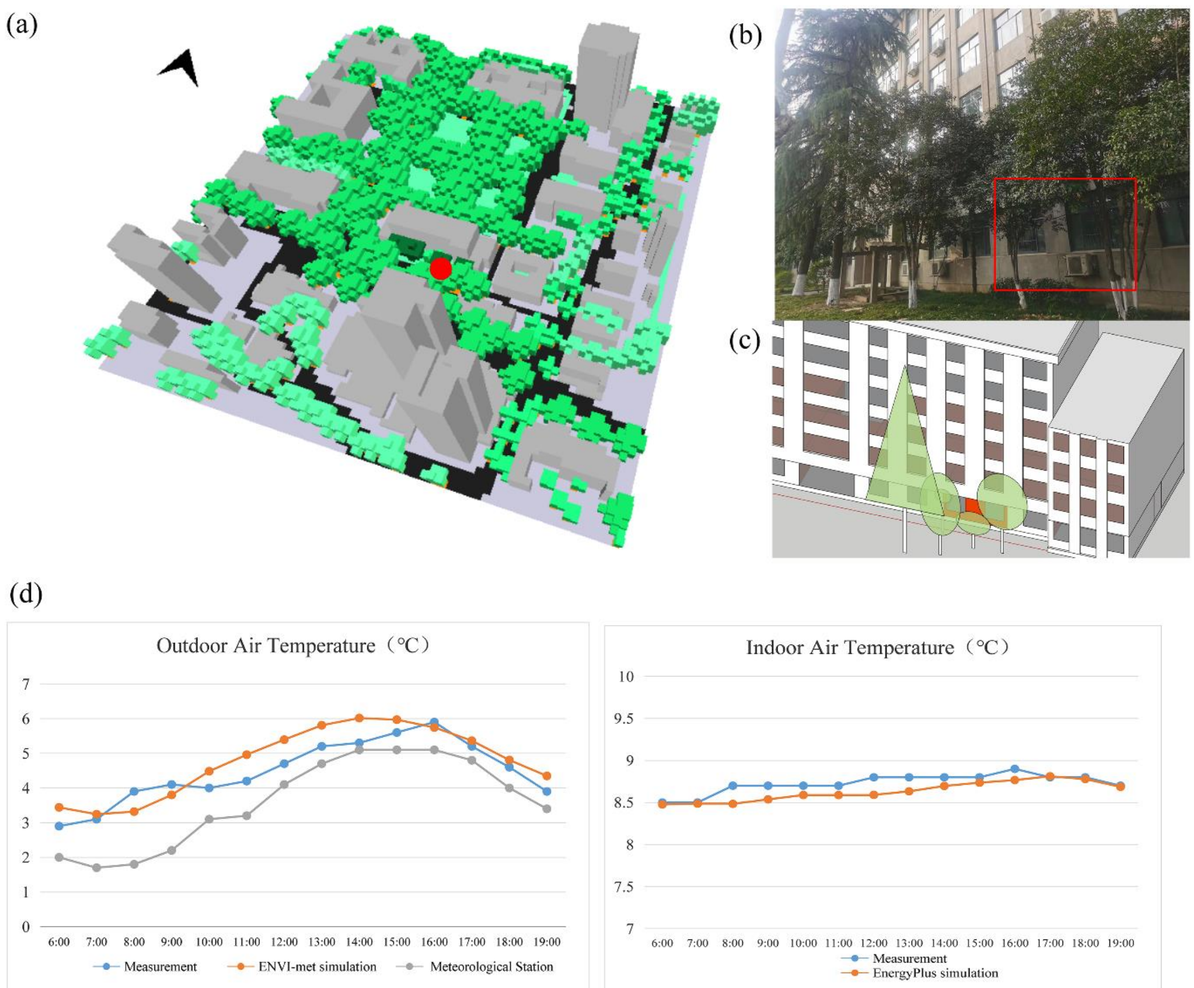

Fig. 8. Modeling of the indoor and outdoor simulation and result comparison of the simulation and measurement.

2.4 Morphological parameters of urban vegetation

Each prototype's vegetation spatial distribution was quantified and then used to analyze the correlation with the urban building energy. This study adopted parameters reflecting the canopy volume of vegetation and its relative spatial relationship with the urban background (Zhu et al., 2020).

Morphological parameters related to urban vegetation, including the mixed standard deviation (*MSD*), aggregation index (*AI*), centripetal index (*CI*), average nearest neighbor (*ANN*) and equilibrium deviation index (*EDI*), are employed. Grid overlay analysis is used to obtain these indices. This study used 30 m × 30 m grids. The calculation of morphological parameters is accomplished in ArcMap 10.5.

MSD is calculated using Equation 1. *MSD* reflects the mixing degree of the vegetation in its located land area. A smaller *MSD* indicates a higher mixing degree of vegetation and its surrounding urban setting, which means that the distribution of vegetation volume in each grid tends to be uniform.

$$MSD = \sqrt{\frac{\sum_{i=1}^{n}(a_i - \bar{a})^2}{n}} \tag{1}$$

where n is the total number of grids, a_i is the ratio of crown volume in the *i*th grid to the area of a single grid, and $\bar{a}$ is the ratio of the total crown volume to land area.

AI is a measure of the degree to which vegetation tends to be concentrated at a point in the site and is calculated with Equations (2) - (6).

k_i and w_i are the grid weight coefficients of vegetation and land, respectively:

$$k_i = \frac{V_i}{V_t} \tag{2}$$

$$w_i = \frac{S_i}{S_t} \tag{3}$$

where S_i is the land area in the *i*th grid, and S_t is the total land area. V_i is the vegetation crown volume in the *i*th grid, and V_t is the total vegetation crown volume. SD_G and SD_L represent the standard distances of vegetation and land:

$$SD_G = \sqrt{\frac{\sum_{i=1}^{n} k_i (x_i - \bar{X})^2}{\sum_{i=1}^{n} k_i} + \frac{\sum_{i=1}^{n} k_i (y_i - \bar{Y})^2}{\sum_{i=1}^{n} k_i}} \tag{4}$$

$$SD_L = \sqrt{\frac{\sum_{i=1}^{n} w_i (x_i - \bar{x})^2}{\sum_{i=1}^{n} w_i} + \frac{\sum_{i=1}^{n} w_i (y_i - \bar{y})^2}{\sum_{i=1}^{n} w_i}} \tag{5}$$

where the coordinates of the *i*th grid center point are (x_i, y_i). The weighted geometric center coordinates of vegetation are ($\bar{X}$,$\bar{Y}$), and the weighted geometric center coordinates of the land area are ($\bar{x}$,$\bar{y}$). *n* is the total number of grids.

$$AI = 2 - \frac{SD_G}{SD_L} \tag{6}$$

The higher the *AI* is, the more concentrated the vegetation; the closer the *AI* is to 1, the closer the vegetation is to a fully balanced state. Vegetation tends to be discrete and edge distributed when *AI* is less than 1. *EDI* is used to quantify the degree of deviation between vegetation form and the fully balanced state (the degree of *AI* deviation from 1):

$$EDI = |1 - AI| \tag{7}$$

CI reflects the degree to which the geometric center point of vegetation is close to the center point of the site. *CI* is calculated as Equation 8:

$$CI = 2 - \frac{\sqrt{(\bar{x} - \bar{X})^2 + (\bar{y} - \bar{Y})^2}}{SD_L} \tag{8}$$

Figure 9 illustrates the graphic changes in *MSD*, *AI*, and *CI* from low to high. *ANN* is calculated as the average value of the distances from each building to the nearest vegetation. The values of each morphological parameter per prototype are included in the Supplementary Information.

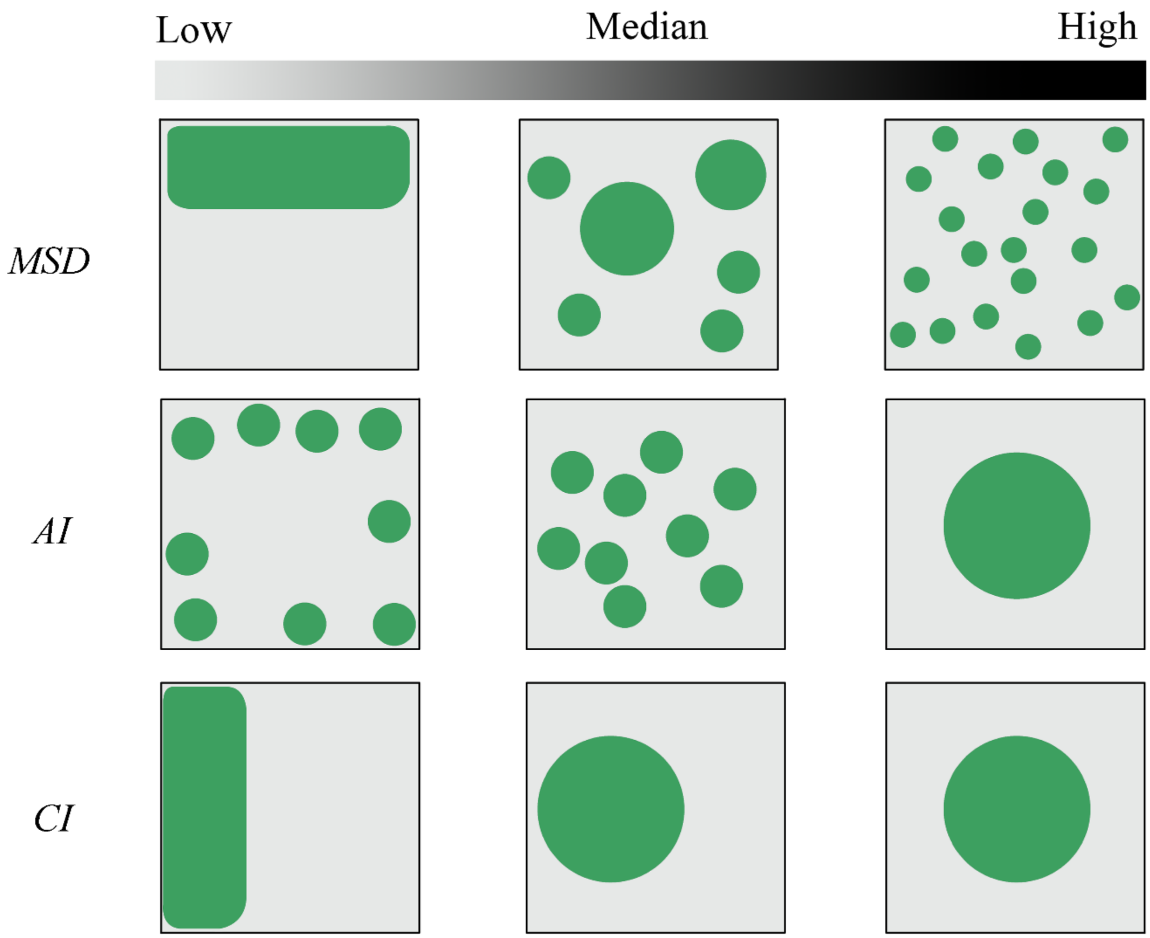

Fig. 9. The graphic characteristics changes of the *MSD*, *AI*, and *CI* from low to high.

3 Results

3.1 Impact of urban vegetation morphology on urban microclimate

The correlation between the microclimate and the vegetation morphological parameters was analyzed for each prototype. The spatial distribution of air temperature and the average microclimate in each prototype in ENVI-met are presented in the Supplementary Information. Table 8 shows the statistics of the correlation between the microclimate and the vegetation morphological parameters. The following conclusions can be drawn:

- MSD is the most significant influencing parameter on the microclimate. This influence is consistent in winter and summer. As the mixing degree of vegetation with its surrounding urban setting increases, the air temperature and wind speed decrease, while the humidity increases. This trend is more prominent in summer than that in winter.
- In summer, the vegetation close to the buildings does not provide much cooling effect to the ambient environment but significantly increases the humidity.
- Concentrated vegetation provides a weaker cooling effect and decreases the humidity.
- Evenly distributed vegetation decreases the wind speed.
- The impact of the vegetation morphological parameters on the microclimate is more significant in summer than winter.

Friedman’s rank test was conducted on the microclimate of the centralized vegetation types in four directions. Significant differences were noted in summer but not in winter. In summer, the east centralized vegetation produces the most significant cooling, humidification, and wind speed reduction effects, followed by the south centralized vegetation. This is due to the prevailing southeast monsoon in summer. In winter, although the centralized vegetation on the east side slightly reduces the wind speed, it dramatically increases the air humidity.

Table 8

Correlation statistics for microclimate and vegetation morphological parameters.

		ANN		*MSD*		*AI*		*CI*		*EDI*	
		R	P	R	P	R	P	R	P	R	P
Summer	Air temperature	0.21	0.202	0.48	0.002 **	0.38	0.016 *	-0.14	0.398	0.20	0.210
	Relative humidity	-0.44	0.004 **	-0.42	0.007 **	-0.37	0.019 *	0.35	0.028 *	-0.30	0.063
	Wind speed	0.3	0.057	0.55	0.000 ***	0.31	0.053	-0.17	0.284	-0.45	0.004 **

Winter	Air temperature	-0.25	0.116	0.37	0.019*	-0.03	0.840	0.27	0.095	-0.03	0.850
	Relative humidity	-0.24	0.128	-0.35	0.026*	-0.20	0.223	0.14	0.374	-0.25	0.125
	Wind speed	0.17	0.285	0.39	0.014*	0.19	0.240	-0.07	0.675	-0.34	0.033*

The significance at the 0.05, 0.01 and 0.001 levels is marked by *, ** and ***, respectively.

3.2 Impact of urban vegetation morphology on urban building energy

3.2.1 Energy performance difference among basic types

The urban building energy consumptions of the basic types were compared and significant differences were noted, as shown in Figure 10. In summer, relatively low energy consumption is associated with the LHH (group 2) and the HHL (group 5). The LLH (group 1) and LHL (group 3) consumes the most energy. The urban form with the characteristic of high density, high rise and high greening ratio produces energy saving effect in summer because it provides significant solar radiation shielding to buildings. However, the pattern is reversed in winter. The energy consumption of the high-rise prototypes is significantly higher than that of the low-rise prototypes in winter. The LHH prototype shows relatively good energy performance in both summer and winter, while the high-rise low-density types perform low energy efficiency in both seasons.

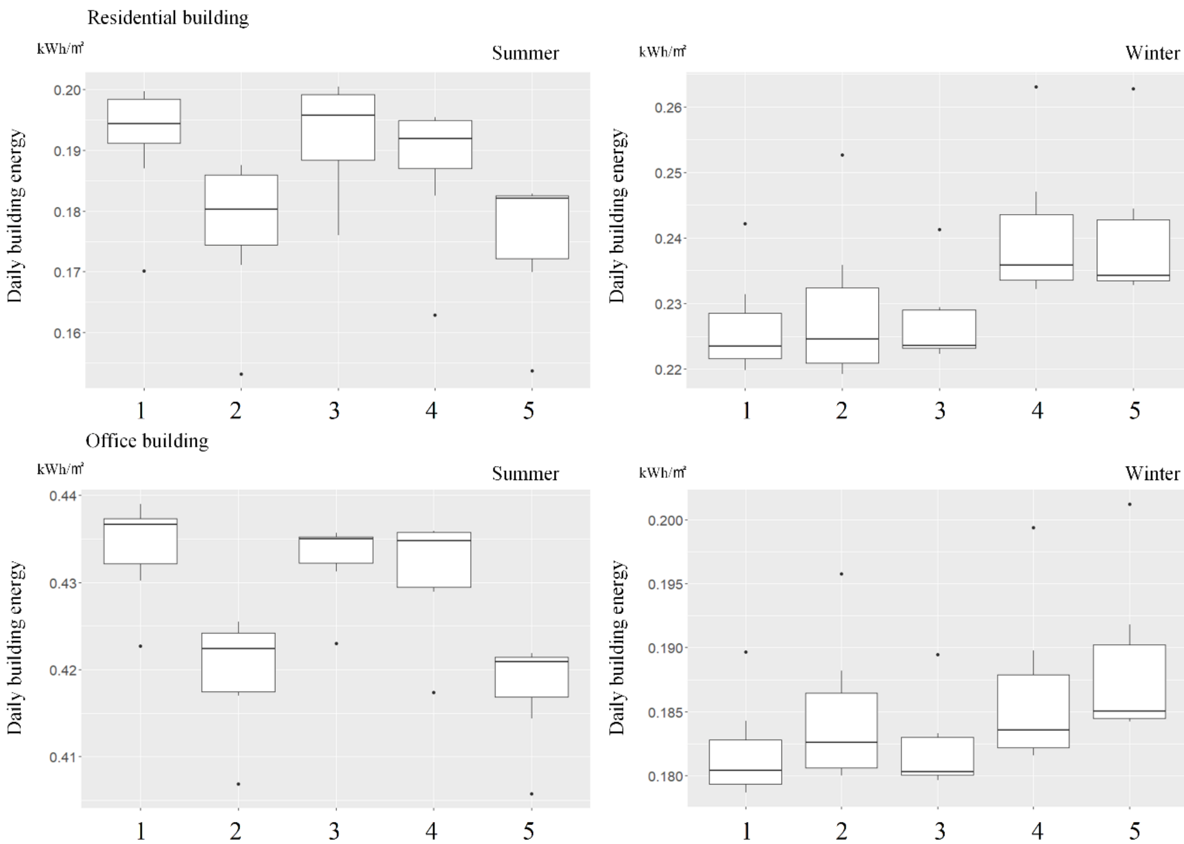

1.Low-rise low-density high-greening ratio; 2.Low-rise high-density high-greening ratio; 3.Low-rise high-density low-greening ratio; 4.High-rise low-density high-greening ratio; 5.High-rise high-density low-greening ratio.

Fig. 10. Comparison of daily energy consumption of different basic types.

3.2.2 Energy performance difference among vegetation spatial distributions

Figure 11 compares the energy consumption of the prototypes with different vegetation spatial distributions. In summer, the energy savings of the prototypes with uniform vegetation spatial distribution are most significant, followed by the prototypes with grouping and surrounding vegetation spatial distributions. The energy-saving effect of the prototype with centralized vegetation spatial distribution is generally weak, while the middle-centralized ones perform slightly better than the side-centralized ones. The energy performance of the prototypes in winter was the opposite of that in summer. For the prototypes with centralized vegetation, no significant difference was found among the four directions.

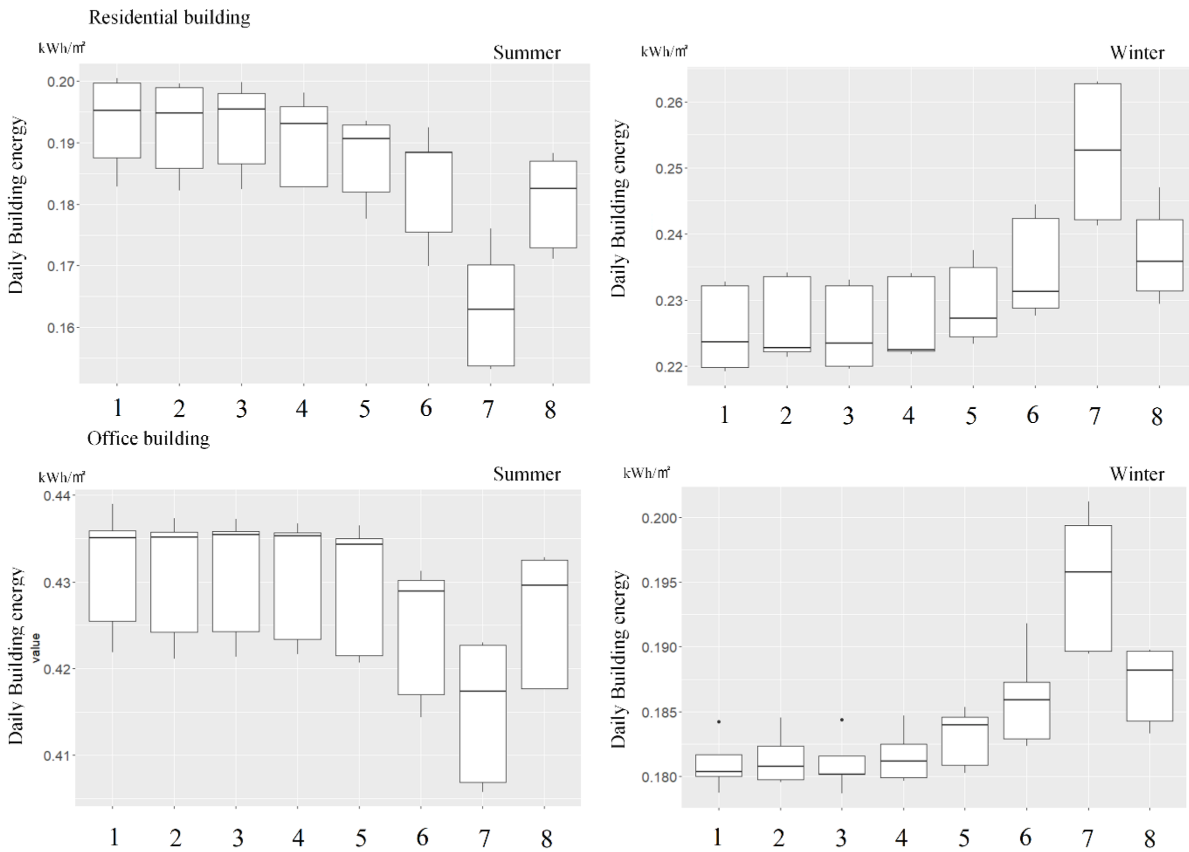

1.South-concentrated; 2. East-concentrated; 3. North-concentrated; 4. West-concentrated; 5. Middle-concentrated; 6. Surrounding; 7.Uniform 8.Grouping.

Fig. 11. Comparison of daily energy consumption of different spatial distributions.

The Z-score of urban building energy consumption of each prototype in its basic type group was calculated to eliminate the influence of buildings and the greening ratio, as shown in Figure 12. After data standardization, the Z-Score distribution of each basic morphological type shows a similar pattern. It indicates that no matter how the building density, height and greening ratio of a block change, the influence of vegetation spatial distribution on urban building energy consumption is similar. Between the energy consumption of residential buildings and that of office buildings, the standardized results are almost the same in winter but slightly different in summer. The urban building energy consumption gap between centralized and uniform distributions is more significant for office buildings in summer.

Fig. 12. The Z-score of daily building energy consumption per floor area of each basic type.

3.2.3 Correlation between vegetation morphological parameters and building energy consumption

Regression analysis was conducted between vegetation morphological parameters and daily urban building energy per floor area. Figure 13 shows the regression results of *ANN*, *MSD*, *CI* and *EDI* with residential building daily energy use. The four morphological parameters are significantly correlated with urban building energy. Analysis of the data in the summer leads to the following findings:

- The results suggested a positive correlation between urban building energy and the average nearest distance between vegetation and buildings. Although Section 3.1 confirms that the vegetation adjacent to the buildings does not reduce the air temperature in the surrounding area of the buildings; however, it provides a considerable shade for the building surfaces and thus reduces the energy use in summer.

- The higher the mixing degree of vegetation and its surrounding urban setting, the less energy is consumed by buildings. The highly mixed vegetation reduces the air temperature surrounding the buildings and provides solar radiation shelter. Vegetation separated from buildings weakens this effect.
- Compared with the layout with vegetation close to the site center, the vegetation distributed on one side provides a weaker cooling effect and shade to the buildings, resulting in more building energy consumption. The greater the vegetation deviates from the site center, the lower the energy efficiency.
- Energy is saved to the maximum extent when the distribution of vegetation in the site tends to be fully balanced. Fully concentrated or surrounding vegetation layouts are disadvantageous for energy savings.

The correlation between *AI* and building energy is weaker than other parameters (shown in the Supplementary Information). The results show that the energy-saving benefit of vegetation with greater dispersion is higher than that of concentrated vegetation in summer.

In winter, the results are opposite to that in summer. The non-equilibrium, separated from the building, and side-concentrated vegetation reduce building energy consumption. The same findings are shown in office prototypes (Figure 14).

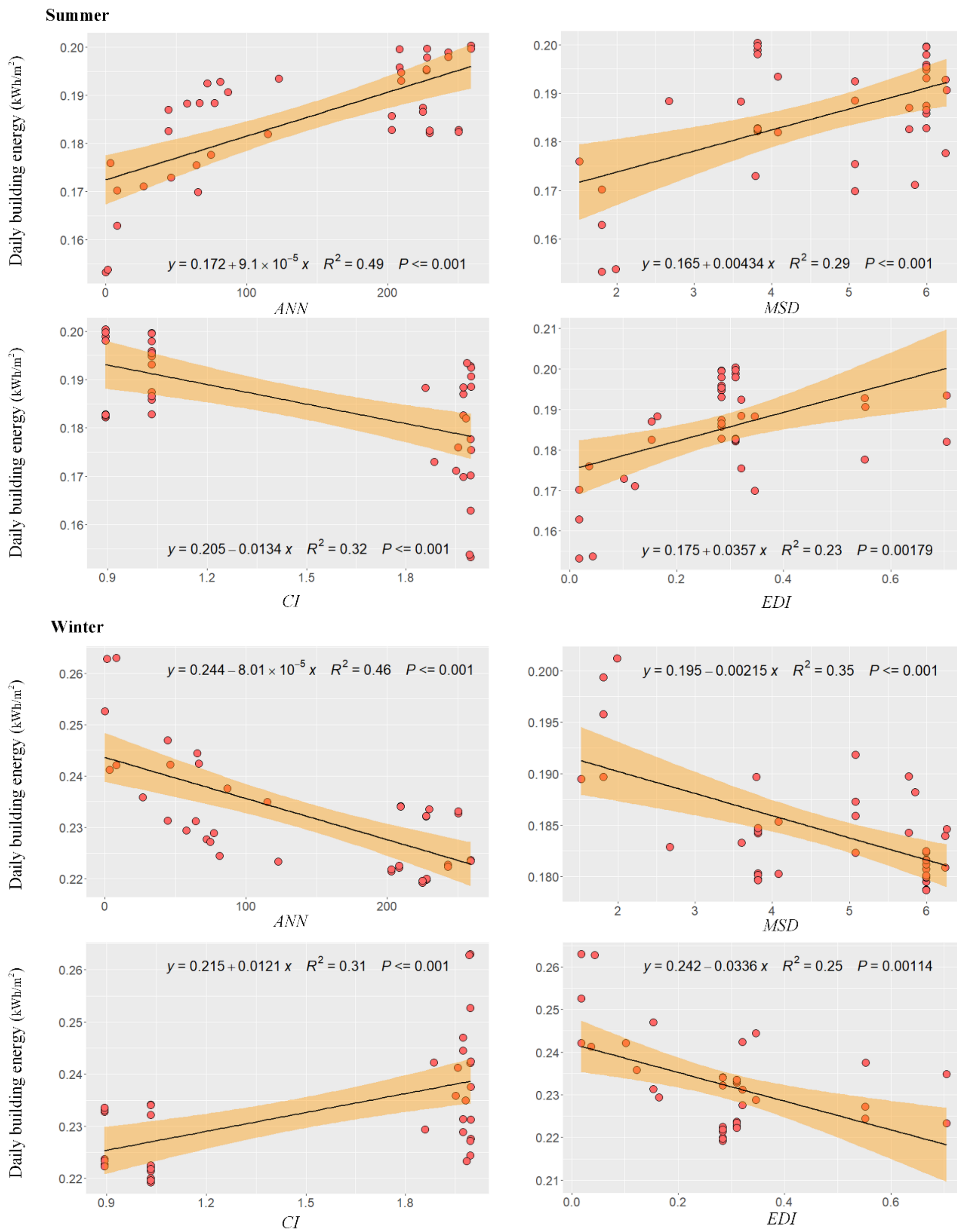

Fig. 13. Correlation between vegetation morphological parameters and residential building energy.

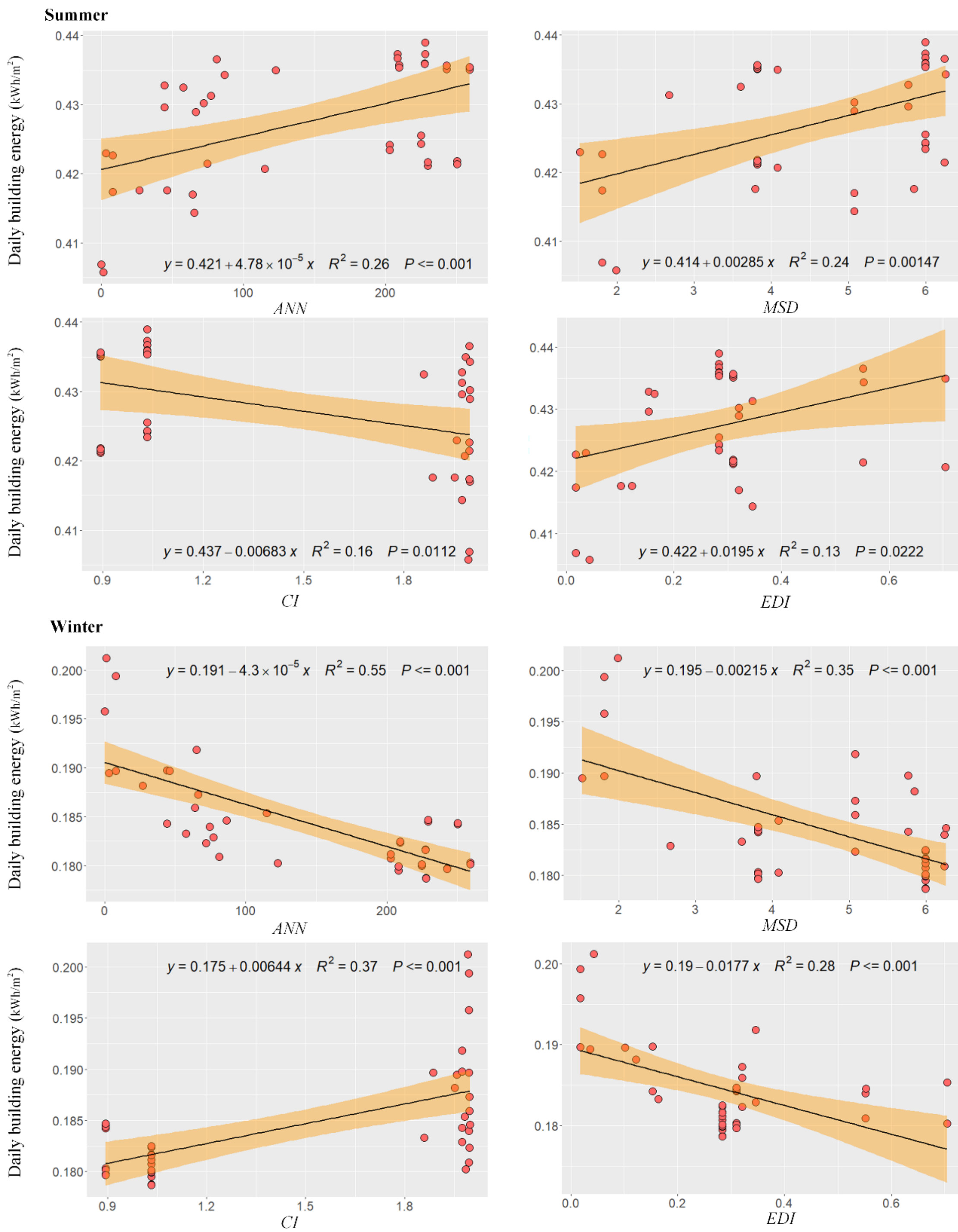

Fig. 14. Correlation between vegetation morphological parameters and office building energy.

3.3 Energy performance difference in summer and winter

The energy results in winter and summer are negatively correlated (Figure 15). However, according to the slope of the fitting equation, the energy consumption difference caused by vegetation morphological change in summer is more substantial than that in winter. It indicates that the energy savings in summer obtained through morphological design are larger than the energy loss caused in winter with similar heating and cooling times. A seasonal comparison of energy consumption in office prototypes indicated a much sharper disparity. As the heat gain from the interior (the heat dissipation of the human body, the heat dissipation of equipment and lighting lamps used) of public buildings is more than residential buildings, the demand for cooling accounts for a larger proportion of the total energy consumption. In contrast, the demand for heating accounts for a smaller proportion. Therefore, adopting a vegetation morphology reduce building energy in summer will benefit public buildings more.

Fig. 15. Correlation between urban building energy in summer and winter.

The correlation between the urban microclimate and urban building energy was analyzed. Table 9 shows the correlation between the average microclimate and the daily energy of residential prototypes, which shows consistency in the office prototypes. In summer, building energy is significantly correlated with the microclimate under the influence of vegetation. It can be attributed to the double-positive energy-saving effect provided by the cooling effects and solar radiation shielding provided by vegetation. However, there is no significant correlation between microclimate and building energy in winter.

The results explain why the change in energy caused by vegetation morphology is more significant in summer than in winter to a certain extent: (a) in summer, the change in vegetation morphology causes more drastic changes in microclimate; thus, the influence of microclimate on urban building energy is more remarkable; (b) due to the decrease in leaf area of deciduous trees, less solar radiation is blocked by the vegetation in winter compared with that in summer.

Table 9

Correlation between microclimate and residential building energy.

		R	Standard Error	P
Summer	Air temperature	0.55	0.065	0.000***
	Relative humidity	-0.64	0.011	0.000 ***
	Wind speed	0.21	0.059	0.192
Winter	Air temperature	0.15	0.096	0.359
	Relative humidity	0.15	0.014	0.343
	Wind speed	0.03	0.094	0.866

The significance at the 0.05, 0.01 and 0.001 levels is marked by *, ** and ***, respectively.

For urban vegetation designers, the opposite effect of urban vegetation morphology on urban building energy in summer and winter may be a depressing conclusion: it suggests that there is no way to adopt an energy-saving scheme in all seasons. However, we can make more favorable choices after comparing the city's energy demand for cooling and heating. Since energy savings are more significant in summer through the vegetation morphology, the vegetation forms beneficial to saving cooling energy are better choices in hot summer/cold winter zones.

4 Discussion

4.1 *Energy-saving potential of urban vegetation morphology*

Quantifying the extent of the influence of urban vegetation morphology on urban building energy is an essential objective of this study, whose results demonstrated a significant impact of urban vegetation morphology on urban building energy. The maximum difference in daily energy consumption of residential buildings in summer and winter was found to be 0.049kWh/m^2 and 0.040kWh/m^2, respectively, accounting for 26.4% and 17.4% of the average total energy consumption of all prototypes. Since the daily running time of office buildings is shorter than that of residential buildings, the daily accumulated change of energy consumption affected by urban vegetation form is relatively weaker than that of residential buildings. The maximum difference in the daily energy consumption of office buildings in summer and winter was found to be 0.032kWh/m^2 (7.4%) and 0.021kWh/m^2 (11.3%). Overall, the daily building energy consumption per floor area can be reduced by 7% ~ 26% by adopting proper vegetation forms. Considering that this reduction represents an average situation for thousands and even tens of thousands of urban buildings, the total energy savings at the whole city level can be tremendous. This finding confirms once again that designing and realizing a proper urban vegetation form is critical for achieving energy-efficient and low-carbon cities.

4.2 *Applicability of the methodology and results to larger scales of urban districts*

The co-simulation technique relies on the widely used and validated building energy and microclimate model. The technique can be applied to study the impact on urban building energy of environmental factors, such as vegetation, waterbodies, ground surfaces, and buildings. The co-simulation improves the simulation efficiency through the automatic batch transmission of data between platforms and the filtering of the elements around each simulated object. Therefore, the method is applicable from microscale to macroscale urban areas. However, due to the speed limit of ENVI-met simulation, the time needed will increase as the method is extended to larger districts.

The impact of larger-scale vegetation patches on urban building energy remains to be explored. On the block scale of this analysis, vegetation affects building energy through both microclimate and solar radiation shielding. When considering large-scale public greenspaces (e.g. municipal parks) separated from buildings, the microclimate approach plays a leading role in the energy-saving effect versus the shading effect of vegetation. Considering the limited influence of vegetation on the microclimate in winter, its cooling effect seems more important in terms of energy conservation. Studies have confirmed that large-scale and complex vegetation patches are conducive to reducing the heat islands of surrounding urban areas (Du et al.,2017; Cao, Onishi, Chen, & Imura,2010), thus helping reduce energy savings. However, the extension distance of cooling is limited. Too concentrated vegetation patches lead to some urban blocks being too far away from vegetation, which weakens its impact on buildings. What size and shape of large-scale public greenspace will have the most positive impact on urban buildings' energy efficiency is a topic worth discussing.

4.3 Potential influences of other morphology factors

Vegetation's evapotranspiration cooling and shading effects depend on the morphological factors associated with tree species, including crown size, leaf area, and seasonal variation. We established typical vegetation models based on the statistics of the main tree species and their average sizes in the study area to reduce the complexity of the simulation. It is impossible to clearly explain the impact of vegetation species on urban building energy through the simplified vegetation model;

however, reasonable inferences can be made. For hot summer/cold winter climate zones and cold climate zones, deciduous vegetation is more beneficial to building energy savings because its seasonal leaf area change provides cooling and shading in summer but reduces the solar radiation blocked in winter. In addition, tall and dense vegetation species perform better in hot climate zones than in cold climate zones.

Physical urban form factors and other natural form factors may interact with vegetation to intensify or weaken the impact of vegetation on urban building energy. The shape, height and density of the buildings affect the solar radiation shielding and microclimate in the site. Other natural elements, including water and soil, produce a local evaporative cooling effect. Further study is required to find the impact of these processes on vegetation's energy effect.

4.4 Limitations

This study presents a quantitative analysis of the correlation between urban building energy and urban vegetation morphology in Nanjing, China. The results provide guidelines for the morphological design of vegetation to reduce urban building energy in the subtropical monsoon climate region. However, the study has limitations worthy of further discussion.

Firstly, the simulation was carried out under local meteorological conditions in Nanjing. Since the impact of vegetation on building energy consumption is significantly affected by meteorological conditions, further research needs to be conducted in other climate regions. Secondly, the urban prototypes were established through the statistics of blocks in Nanjing. The applicability of the conclusions in cities with different urban morphological characteristics, e.g., building height, density, and dominant tree species, should be further validated. In addition, this study uses a unidirectional coupling method from microclimate to building energy simulation. It does not take into account the impact of building heat release on urban microclimate, which requires improved methods and platforms for coupling simulations. Another limitation of the study is that a relatively large grid size in ENVI-met was used. The simulation resolution of ENVI-met is 1–10 m, while the resolution used in this study is 8 m × 8 m × 6 m. This is a relatively coarse resolution, in order to reduce computational resources in large-scale simulations. Last but not least, this study focuses on the impact of vegetation on building energy use and does not analyze the impact of other urban morphological factors, e.g., water bodies, buildings, and surface materials, on urban building energy demand. These limitations can be overcome in the future through improved simulation methods and further simulations and field studies.

5 Conclusions

Urban vegetation is an indispensable part of urban morphology and its impact on building energy consumption is widely recognized. However, how vegetation morphology affects urban building energy at the urban district level and its magnitude requires further investigation. This study aimed to analyze the quantitative relation between urban vegetation morphology and urban building energy and provide support to energy efficient urban morphological strategy. The morphology of Nanjing, China, was statistically analyzed. Based on building density, height, vegetation volume and spatial distribution of vegetation, 40 urban building-vegetation morphological prototypes were extracted. Five morphological parameters were selected to quantify the vegetation spatial features of the prototypes. Using the co-simulation technique, the microclimate and urban building energy of the urban prototypes were simulated. The results indicated a statistically significant correlation between the daily urban building energy per floor area and the urban vegetation morphology. Through the presented results, the following findings could be obtained to guide urban morphological design:

- Adopting the LHH type in urban design can reduce urban building energy throughout the year;

- Low-greening ratio and low-density urban form should be avoided in hot climate zones and hot summer/cold winter zones;
- Extensive use of high-rise blocks should be avoided in cold climate zones;
- The vegetation close to the geometric center of the site, uniformly distributed, and highly mixed with buildings should be adopted in hot climate zones and hot summer/cold winter zones;
- The vegetation distribution concentrated, separated from the building, and deviated from the center of the site should be adopted in cold climate zones.

In the future, studies could be carried out to further tap the potential of urban vegetation morphological design in urban building energy savings. First, the impact of large-scale urban greenspace morphology on urban building energy and its magnitude needs further investigation. Building a microclimate model that is more efficient and suitable for macroscale urban districts and integrating it into the urban building energy simulation workflow is worth exploring. In addition, studies should be conducted on the influence of other urban morphological factors on urban building energy and their cross-impact with vegetation's energy-saving effect. Finally, the authors of this paper would like to extend the co-simulation technique to the application of urban design and planning design workflows, to give urban planners and designers an effective tool to better consider and integrate urban vegetation into their projects.

References:

Balogun, A. A., Morakinyo, T. E., & Adegun, O. B. (2014). Effect of tree-shading on energy demand of two similar buildings. *ENERGY AND BUILDINGS*, 81, 305-315. http://doi.org/https://doi.org/10.1016/j.enbuild.2014.05.046

Bruse, M. (2004). ENVI-met 3.0: updated model overview. *University of Bochum. Retrieved from: www. envi-met. com*

Bruse, M., & Fleer, H. (1998). Simulating surface–plant–air interactions inside urban environments with a three dimensional numerical model. *ENVIRONMENTAL MODELLING & SOFTWARE*, 13(3-4), 373-384.

Chen, L., Letu, H., Fan, M., Shang, H., Tao, J., Wu, L., Zhang, Y., Yu, C., Gu, J., Zhang, N., Hong, J., Wang, Z., & Zhang, T. (2022). An Introduction to the Chinese High-Resolution Earth Observation System: Gaofen-1~7 Civilian Satellites. *Journal of Remote Sensing*, 2022, 9769536. http://doi.org/10.34133/2022/9769536

Crawley, D. B., Lawrie, L. K., Winkelmann, F. C., Buhl, W. F., Huang, Y. J., Pedersen, C. O., Strand, R. K., Liesen, R. J., Fisher, D. E., Witte, M. J., & Glazer, J. (2001). EnergyPlus: creating a new-generation building energy simulation program. *ENERGY AND BUILDINGS*, 33(4), 319-331. http://doi.org/https://doi.org/10.1016/S0378-7788(00)00114-6

DeWalle, D. R., & Heisler, G. M. (1983). Windbreak effects on air infiltration and space heating in a mobile home. *ENERGY AND BUILDINGS*, 5(4), 279-288. http://doi.org/https://doi.org/10.1016/0378-7788(83)90015-4

Donovan, G. H., & Butry, D. T. (2009). The value of shade: Estimating the effect of urban trees on summertime electricity use. *ENERGY AND BUILDINGS*, 41(6), 662-668. http://doi.org/https://doi.org/10.1016/j.enbuild.2009.01.002

Du, H., Cai, W., Xu, Y., Wang, Z., Wang, Y., & Cai, Y. (2017). Quantifying the cool island effects of urban green spaces using remote sensing Data. *URBAN FORESTRY & URBAN GREENING*, 27, 24-31.

Du, S., Zhang, X., Jin, X., Zhou, X., & Shi, X. (2022). A review of multi-scale modelling, assessment, and improvement methods of the urban thermal and wind environment. *BUILDING AND ENVIRONMENT*, 213, 108860.

http://doi.org/https://doi.org/10.1016/j.buildenv.2022.108860

Fumo, N., Mago, P., & Luck, R. (2010). Methodology to estimate building energy consumption using EnergyPlus Benchmark Models. *ENERGY AND BUILDINGS*, 42(12), 2331-2337. http://doi.org/https://doi.org/10.1016/j.enbuild.2010.07.027

Heisler, G. M. (1986). Energy savings with trees. *Journal of Aboriculture. 12 (5): 113-125.*, 12(5), 113-125.

Heisler, G. M. (1990). Mean wind speed below building height in residential neighborhoods with different tree densities. *ASHRAE Transactions. 96 (1): 1389-1396.*, 96(1), 1389-1396.

Hildebrandt, E. W., & Sarkovich, M. (1998). Assessing the cost-effectiveness of SMUD's shade tree program. *ATMOSPHERIC ENVIRONMENT*, 32(1), 85-94. http://doi.org/https://doi.org/10.1016/S1352-2310(97)00183-0

Hong, T., Taylor-Lange, S. C., D Oca, S., Yan, D., & Corgnati, S. P. (2016). Advances in research and applications of energy-related occupant behavior in buildings. *ENERGY AND BUILDINGS*, 116, 694-702. http://doi.org/https://doi.org/10.1016/j.enbuild.2015.11.052

Hwang, W. H., Wiseman, P. E., & Thomas, V. A. (2016). Simulation of shade tree effects on residential energy consumption in four US cities. *Cities and the Environment (CATE)*, 9(1), 2.

IEA. (2015). *Energy Technology Perspectives 2015*. IEA. www.iea.org/etp/etp2015.

Jim, C. Y., & Chen, S. S. (2003). Comprehensive greenspace planning based on landscape ecology principles in compact Nanjing city, China. *LANDSCAPE AND URBAN PLANNING*, 65(3), 95-116. http://doi.org/https://doi.org/10.1016/S0169-2046(02)00244-X

Ko, Y. (2018). Trees and vegetation for residential energy conservation: A critical review for evidence-based urban greening in North America. *URBAN FORESTRY & URBAN*

GREENING, 34, 318-335. http://doi.org/https://doi.org/10.1016/j.ufug.2018.07.021

Ko, Y., & Radke, J. D. (2014). The effect of urban form and residential cooling energy use in Sacramento, California. *Environment and Planning B: Planning and Design*, 41(4), 573-593. http://doi.org/https://doi.org/10.1068/b12038p

Kobayashi, H. (2012). *Forest Light Environmental Simulator for voxel data* Retreved 9 from https://sites.google.com/site/fliesdevelop/users-manual

Kobayashi, H., & Iwabuchi, H. (2008). A coupled 1-D atmosphere and 3-D canopy radiative transfer model for canopy reflectance, light environment, and photosynthesis simulation in a heterogeneous landscape. *REMOTE SENSING OF ENVIRONMENT*, 112(1), 173-185.

Liu, C., Li, Z., Jing, X., Gao, W., Shi, J., Cai, G., & Wang, Y. (2022). Influence of landscape outside the window on the anxiety level of self-separation people during COVID-19. *International Journal of Low-Carbon Technologies*, 17, 678-685. http://doi.org/10.1093/ijlct/ctac041

Liu, Z., Cheng, W., Jim, C. Y., Morakinyo, T. E., Shi, Y., & Ng, E. (2021). Heat mitigation benefits of urban green and blue infrastructures: A systematic review of modeling techniques, validation and scenario simulation in ENVI-met V4. *BUILDING AND ENVIRONMENT*, 200, 107939. http://doi.org/https://doi.org/10.1016/j.buildenv.2021.107939

Mangone, G., Kurvers, S. R., & Luscuere, P. G. (2014). Constructing thermal comfort: Investigating the effect of vegetation on indoor thermal comfort through a four season thermal comfort quasi-experiment. *BUILDING AND ENVIRONMENT*, 81, 410-426. http://doi.org/https://doi.org/10.1016/j.buildenv.2014.07.019

McPherson, E. G., & Rowntree, R. A. (2016). Energy conservation potential of urban tree planting

Meier, A. K. (1990). Strategic landscaping and air-conditioning savings: A literature review. *ENERGY AND BUILDINGS*, 15(3), 479-486. http://doi.org/https://doi.org/10.1016/0378-7788(90)90024-D

Morakinyo, T. E., Dahanayake, K. K. C., Adegun, O. B., & Balogun, A. A. (2016). Modelling the effect of tree-shading on summer indoor and outdoor thermal condition of two similar buildings in a Nigerian university. *ENERGY AND BUILDINGS*, 130, 721-732.

Morakinyo, T. E., Dahanayake, K. W. D. K., Ng, E., & Chow, C. L. (2017). Temperature and cooling demand reduction by green-roof types in different climates and urban densities: A co-simulation parametric study. *ENERGY AND BUILDINGS*, 145, 226-237. http://doi.org/https://doi.org/10.1016/j.enbuild.2017.03.066

Natanian, J., & Auer, T. (2020). Beyond nearly zero energy urban design: A holistic microclimatic energy and environmental quality evaluation workflow. *Sustainable Cities and Society*, 56, 102094. http://doi.org/https://doi.org/10.1016/j.scs.2020.102094

Oke, T. R. (2002). *Boundary layer climates*. Routledge.

Pan, L., Wei, S., Lai, P. Y., & Chu, L. M. (2020). Effect of plant traits and substrate moisture on the thermal performance of different plant species in vertical greenery systems. *BUILDING AND ENVIRONMENT*, 175, 106815. http://doi.org/https://doi.org/10.1016/j.buildenv.2020.106815

Pan, L., Wei, S., & Chu, L. M. (2018). Orientation effect on thermal and energy performance of vertical greenery systems. *ENERGY AND BUILDINGS*, 175, 102-112. http://doi.org/https://doi.org/10.1016/j.enbuild.2018.07.024

Pandit, R., & Laband, D. N. (2010). Energy savings from tree shade. *ECOLOGICAL*

ECONOMICS, 69(6), 1324-1329. http://doi.org/https://doi.org/10.1016/j.ecolecon.2010.01.009

Schipperijn, J., Bentsen, P., Troelsen, J., Toftager, M., & Stigsdotter, U. K. (2013). Associations between physical activity and characteristics of urban green space. *URBAN FORESTRY & URBAN GREENING*, 12(1), 109-116. http://doi.org/https://doi.org/10.1016/j.ufug.2012.12.002

Scott, M. J., Wrench, L. E., & Hadley, D. L. (1994). Effects of climate change on commercial building energy demand. *Energy sources*, 16(3), 317-332.

Seto, K. C., Dhakal, S., Bigio, A., Blanco, H., Delgado, G. C., Dewar, D., Huang, L., Inaba, A., Kansal, A., & Lwasa, S. (2014). Human settlements, infrastructure and spatial planning

Shi, Z., Fonseca, J. A., & Schlueter, A. (2017). A review of simulation-based urban form generation and optimization for energy-driven urban design. *BUILDING AND ENVIRONMENT*, 121, 119-129. http://doi.org/https://doi.org/10.1016/j.buildenv.2017.05.006

Shinzato, P., Simon, H., Silva Duarte, D. H., & Bruse, M. (2019). Calibration process and parametrization of tropical plants using ENVI-met V4–Sao Paulo case study. *Architectural Science Review*, 62(2), 112-125. http://doi.org/https://doi.org/10.1080/00038628.2018.1563522

Simon, H., Lindén, J., Hoffmann, D., Braun, P., Bruse, M., & Esper, J. (2018). Modeling transpiration and leaf temperature of urban trees–a case study evaluating the microclimate model ENVI-met against measurement data. *LANDSCAPE AND URBAN PLANNING*, 174, 33-40. http://doi.org/https://doi.org/10.1016/j.landurbplan.2018.03.003

Simpson, J. R. (1998). Urban forest impacts on regional cooling and heating energy use:

Sacramento County case study. *Journal of Arboriculture*, 24, 201-214.

Simpson, J. R. (2002). Improved estimates of tree-shade effects on residential energy use. *ENERGY AND BUILDINGS*, 34(10), 1067-1076. http://doi.org/https://doi.org/10.1016/S0378-7788(02)00028-2

Simpson, J. R., & McPherson, E. G. (1996). Potential of tree shade for reducing residential energy use in California. *Journal of Arboriculture. 22 (1): 10-18*, 22(1), 10-18.

Stewart, I. D., & Oke, T. R. (2012). Local climate zones for urban temperature studies. *BULLETIN OF THE AMERICAN METEOROLOGICAL SOCIETY*, 93(12), 1879-1900.

Thayer, R. L., Zanetto, J., & Maeda, B. T. (1983). Modeling the effects of street trees on the performance of solar and conventional houses in Sacramento, California. *Landscape Journal*, 2(2), 155-164.

Tian, Z., Zhang, X., Jin, X., Zhou, X., Si, B., & Shi, X. (2018). Towards adoption of building energy simulation and optimization for passive building design: A survey and a review. *ENERGY AND BUILDINGS*, 158, 1306-1316. http://doi.org/https://doi.org/10.1016/j.enbuild.2017.11.022

U.S. Department of Energy. (2021). *EnergyPlus Version 9.6.0 Documentation Input Output Reference*. U.S. Department of Energy.

US Department of Energy. (2015). An assessment of energy technologies and research opportunities. *Quadrennial Technology Review*, 145.

Yang, X., Zhao, L., Bruse, M., & Meng, Q. (2012). An integrated simulation method for building energy performance assessment in urban environments. *ENERGY AND BUILDINGS*, 54, 243-251.

Zhou, X., Liu, T., Shi, X., & Jin, X. (2018). Case study of window operating behavior patterns in an open-plan office in the summer. *ENERGY AND BUILDINGS*, 165, 15-24. http://doi.org/https://doi.org/10.1016/j.enbuild.2018.01.037

Zhou, X., Ren, J., An, J., Yan, D., Shi, X., & Jin, X. (2021). Predicting open-plan office window operating behavior using the random forest algorithm. *Journal of Building Engineering*, 42, 102514. http://doi.org/https://doi.org/10.1016/j.jobe.2021.102514

Zhu, D., Hong, T., Yan, D., & Wang, C. (2013). A detailed loads comparison of three building energy modeling programs: EnergyPlus, DeST and DOE-2.1E. *Building Simulation*, 6(3), 323-335. http://doi.org/10.1007/s12273-013-0126-7

Zhu, S., Du, S., Li, Y., Wei, S., Jin, X., Zhou, X., & Shi, X. (2020). A 3D spatiotemporal morphological database for urban green infrastructure and its applications. *URBAN FORESTRY & URBAN GREENING*, 126935. http://doi.org/https://doi.org/10.1016/j.ufug.2020.126935

Zhu, S., Yang, Y., Yan, Y., Causone, F., Jin, X., Zhou, X., & Shi, X. (2022). An evidence-based framework for designing urban green infrastructure morphology to reduce urban building energy use in a hot-humid climate. *BUILDING AND ENVIRONMENT*, 219, 109181. http://doi.org/https://doi.org/10.1016/j.buildenv.2022.109181